Published in final edited form as:
*Neuron*. 2011 October 6; 72(1): 178–187. doi:10.1016/j.neuron.2011.08.010.

# Olfactory Predictive Codes and Stimulus Templates in Piriform Cortex

**Christina Zelano**[1,*], **Aprajita Mohanty**[2], and **Jay A. Gottfried**[1]

[1]Department of Neurology, Feinberg School of Medicine, Northwestern University, Chicago, IL 60611, USA

[2]Department of Psychology, Stony Brook University, Stony Brook, NY, 11794, USA

## Summary

Neuroscientific models of sensory perception suggest that the brain utilizes predictive codes in advance of a stimulus encounter, enabling organisms to infer forthcoming sensory events. However, it is poorly understood how such mechanisms are implemented in the olfactory system. Combining high-resolution functional magnetic resonance imaging with multivariate (pattern-based) analyses, we examined the spatiotemporal evolution of odor perception in the human brain during an olfactory search task. Ensemble activity patterns in anterior piriform cortex (APC) and orbitofrontal cortex (OFC) reflected the attended odor target both before and after stimulus onset. In contrast, pre-stimulus ensemble representations of the odor target in posterior piriform cortex (PPC) gave way to post-stimulus representations of the odor itself. Critically, the robustness of target-related patterns in PPC predicted subsequent behavioral performance. Our findings directly show that the brain generates predictive templates or "search images" in PPC, with physical correspondence to odor-specific pattern representations, to augment olfactory perception.

## Introduction

The process by which the brain transforms sensory inputs into perceptual events often begins before physical contact with the sensory stimulus (Freeman, 1979; Friston, 2005; McMains et al., 2007; Mesulam, 2008; Mumford, 1992; Sylvester et al., 2009; Wald and Wolfowitz, 1949). Knowledge and experience set expectations for what is likely – but not yet – to be encountered, helping to augment the speed and accuracy of subsequent perceptual judgments. These predictive representations confer distinct behavioral advantages upon organisms aiming to survive in complex, noisy, and unpredictable sensory environments.

How predictive perceptual information is encoded in the brain is not well understood. Several influential models of sensory perception have centered on the idea that the brain generates stimulus templates or "search images" in advance of a stimulus encounter (Freeman, 1981; Friston, 2003; Mumford, 1992). According to such mechanisms a sensory percept is instantiated through an interaction between the pre-stimulus template and the incoming sensory input. Multiple studies have found effects of anticipatory attention in the



*To whom correspondence should be addressed: c-zelano@northwestern.edu, Phone: 312-503-3086.

visual and auditory systems (Kastner et al., 1999; Kumar et al., 2011; Luck et al., 1997; Ress et al., 2000), and more recently effects of anticipatory attention or top-down search have also been found for specific visual objects in higher-order visual cortex (Esterman and Yantis, 2010; Peelen et al., 2009; Stokes et al., 2009; Summerfield et al., 2006).

By comparison, research on predictive coding in the olfactory system has been scant at best. Given that odor objects are routinely experienced within a highly odiferous background (Gottfried, 2010; Stevenson and Wilson, 2007), it follows that mechanisms to steer selective attention toward an odor of interest, and away from an odor of no interest, would be essential for overcoming sensory noise in the olfactory environment. In an early model of olfactory perception (Freeman, 1981), Walter Freeman postulated that spatiotemporally distributed “search images” in the rabbit olfactory bulb provide an active filter that selectively enhances perceptual sensitivity to expected odors, without impairing responsiveness to unattended odors (Freeman, 1983). He concluded that “rabbits smell what they expect, not what they sniff.” More recent electrophysiological recordings in rodents have identified pre-stimulus anticipatory events not only in the bulb, but also in piriform cortex and orbitofrontal cortex (Kay and Freeman, 1998; Schoenbaum and Eichenbaum, 1995), implying that well before an odor arrives, much of the olfactory system generates a prediction about the upcoming stimulus. Finally, in human piriform cortex, attention to olfactory content evokes baseline deviations in fMRI activity (Zelano et al., 2005), though it is unclear whether these changes merely reflect a general attentional gain, or reflect feature-based predictive codes about specific odors.

Olfactory studies in humans and other animals increasingly show that cortical representations of odor in piriform cortex are encoded as spatially distributed ensembles (Freeman, 1979; Haberly, 1985; Haberly, 2001; Hasselmo et al., 1990; Howard et al., 2009; Illig and Haberly, 2003; Kay and Stopfer, 2006; Martin et al., 2004; Spors and Grinvald, 2002; Stettler and Axel, 2009; Wilson and Stevenson, 2003) evolving over a time-span of seconds (Rennaker et al., 2007). Therefore, based on these observations, we combined an olfactory attentional search task with functional magnetic resonance imaging (fMRI) techniques and pattern-based multivariate analyses to test three hypotheses following from the predictive coding model: (1) odor-specific predictive codes in the human olfactory brain are established prior to stimulus onset and take the form of spatially distributed templates or “search images”; (2) ensemble activity patterns should evolve in space and time over the course of a trial, such that predictive coding gives way to stimulus coding from pre- to post-odor onset; and (3) a legitimate pre-stimulus predictive template should be able to predict olfactory behavioral performance in the post-stimulus period.

Subjects participated in a simple olfactory fMRI task in which they decided whether a particular pre-determined target smell was present on each trial. In target A runs, subjects determined whether or not odor A was present, and in target B runs, subjects determined whether or not odor B was present. Stimuli consisted of either odor A alone (A), odor B alone (B), or a binary mixture of odors A and B (AB), resulting in six conditions: target **A** with stimulus A, B, or AB (**A**|A, **A**|B, **A**|AB), and target **B** with stimulus A, B, or AB (**B**|A, **B**|B, **B**|AB) (Fig. 1). Importantly, the physical characteristics of the stimuli were identical across runs, ensuring that the only differing aspect between target A and target B runs was the attentional focus of the subject. By comparing conditions with the *target* held constant, to conditions with the *stimulus* held constant, we were able to look for target-related and stimulus-related activity patterns, and observe how those patterns evolved from pre- to post-stimulus. Principal regions of interest (ROIs) included anterior piriform cortex (APC), posterior piriform cortex (PPC), orbitofrontal cortex (OFC), and mediodorsal thalamus (MDT), areas that have been previously implicated in human imaging studies of odor quality coding (Gottfried et al., 2006; Howard et al., 2009), odor imagery (Bensafi et al., 2007;

Djordjevic et al., 2005), odor localization (Porter et al., 2005), olfactory working memory (Zelano et al., 2009), and olfactory and gustatory attentional modulation (Plailly et al., 2008; Veldhuizen et al., 2007; Zelano et al., 2005).

## Results

### Olfactory selective attention biases behavioral performance and enhances response times

During a given target run (either A or B), subjects were cued to sniff and to indicate as accurately and quickly as possible whether the odor stimulus (either A, B, or AB) contained the target note. Behavioral data were analyzed using a two-way repeated-measures ANOVA, with factors "target" (2 levels) and "stimulus" (3 levels). There was no main effect of target on performance accuracy: subjects identified the target equally well on both A and B runs ($F_{1,11}$ = 0.54; $P$ = 0.478) (Fig. 2A). In contrast, a significant main effect of odor stimulus was observed ($F_{1.83,20.11}$ = 10.08; $P$ = 0.001), whereby subjects were less accurate on stimulus AB trials than on stimulus A and B trials (A vs. AB: $T_{11}$ = 4.39, $P$ = 0.001; B vs. AB: $T_{11}$ = 3.96, $P$ < 0.002).

Interestingly, although mean accuracy was comparable for A and B odor stimuli ($T_{11}$ = 0.46, $P$ = 0.6), there was a significant stimulus-by-target interaction ($F_{1.88,20.67}$ = 8.951; $P$ = 0.002), such that accuracy on target A runs was higher (at trend) for stimulus A than for stimulus B ($T_{11}$=2.0, $P$ < 0.07), and accuracy on target B runs was higher for stimulus B than for stimulus A ($T_{11}$=4.0, $P$ < 0.002) (Fig. 2A). In other words, subjects made fewer errors on *congruent* trials in which the target was present in the stimulus (i.e., **A**|A and **B**|B), compared to *incongruent* trials in which the target was not present (i.e., **A**|B and **B**|A). This effect is summarized in Fig. 2B (congruent vs. incongruent: $T_{11}$=3.35, $P$ < 0.006). Moreover, reaction times were significantly faster on congruent trials when the target note was present in the stimulus compared to incongruent trials when it was not ($T_{11}$ = 3.01, $P$ < 0.01) (Fig. 2C), highlighting the effect of our attentional manipulation on behavior. While several studies have found evidence for a general effect of attending to olfactory versus non-olfactory sensory modalities (Plailly et al., 2008; Sabri et al., 2005; Spence et al., 2001; Zelano et al., 2005), our results imply that selective attention within the olfactory modality also exists, which has been previously debated (Laing and Glemarec, 1992; Takiguchi et al., 2008).

Due to the known influence of sniffing on olfactory activation patterns in humans (Sobel et al., 1998), we also examined condition-specific respiratory patterns across subjects, and confirmed that there was no effect of attended target ($F_{1,11}$ = 1.007, $P$ = 0.159), odor stimulus ($F_{1,11.01}$ = 0.73, $P$ =0.411), or target-by-stimulus interaction ($F_{1,11}$ = 0.914, $P$ = 0.36) on inspiratory sniff volume (data not shown). Thus, the only salient cognitive difference between target A and target B runs was the attentional focus of the subject.

### Pre-stimulus ensemble patterns in olfactory cortex reflect the odor target

We first examined whether odor-specific ensemble patterns were formed prior to the arrival of the stimulus. The central hypothesis was that prior to odor onset, spatial activity patterns would be more correlated between *same-target* conditions than between *different-target* conditions in brain regions encoding the odor target. Thus for example, if a given ROI reflected the targeted note, the pre-stimulus pattern in response to condition **A**|A would correlate more strongly to **A**|B (same target but different stimulus) than to **B**|A (different target but same stimulus). Conversely, in a region encoding the actual odor stimulus, the pattern in response to condition **A**|A would correlate more strongly to **B**|A (same stimulus but different target) than to **A**|B (different stimulus but same target). In this manner, a distinct contrast (same target/different stimulus correlations vs. same stimulus/different

target correlations) could be tested to look for both target-related and stimulus-related effects, both before and after odor onset (Fig. 3A). These analyses were computed for target A runs and for target B runs in the pre-and post-stimulus time bins, and entered into a 3-way repeated-measures ANOVA with the factors "target run" (A or B), "pattern type" (target-related or stimulus-related pattern), and "time" (pre- or post-stimulus onset). Because no region exhibited a significant effect of target run (all *P's* > 0.2), data are shown collapsed across A and B runs (for non-collapsed data, see Fig. S1).

In line with the idea that pre-stimulus, odor-specific patterns exist in the olfactory system, fMRI ensemble correlations between same-target conditions were significantly higher than correlations between different-target conditions (Fig. 3B). In APC and OFC, there was a significant effect of pattern type (APC: $F_{1,11}$=30.933, $P < 0.0001$; OFC: $F_{1,11} = 13.437$, $P < 0.004$) in the target direction, whereby same-target conditions were more correlated than different-target conditions (APC: $T_{11} = 5.6$, $P < 0.0001$; OFC: $T_{11} = 3.67$, $P < 0.003$). In APC, there was also a significant pattern type-by-time interaction ($F_{1,11} = 5.79$, $P < 0.035$) in which the same-target (compared to different-target) correlations were larger in the pre-stimulus bin than in the post-stimulus bin (pre: $T_{11} = 6.3$, $P < 0.0001$; post: $T_{11} = 1.99$, $P < 0.07$). There was no such interaction in OFC ($P = 0.3$). Neither MDT nor PPC exhibited a significant main effect of pattern type or time (*P*'s > 0.1).

## fMRI patterns in PPC evolve from pre-stimulus target representations to post-stimulus odor representations

Although PPC exhibited no main effect of pattern type (either in the target direction or the stimulus direction), there was a significant pattern type-by-time interaction ($F_{1,11} = 22.702$, $P < 0.001$). Follow-up t-tests revealed a double dissociation, such that same-target conditions were more correlated than different-target conditions *before* stimulus onset ($T_{11} = 2.6$, $P < 0.02$), but same-stimulus conditions were more correlated than different-stimulus conditions *after* stimulus onset ($T_{11} = -5.45$, $P < 0.001$) (Fig. 3B).

To directly visualize how the informational content of the fMRI signal changes over time and across different regions, we plotted the mean correlations between same-target conditions (e.g., **A**|A to **A**|B) and between same-stimulus conditions (e.g., **A**|A to **B**|A), separately for each time-point in the trial (Fig. 4). Within APC and OFC, target-specific patterns emerged early in the pre-stimulus period, and in the case of APC this effect significantly persisted for several seconds into the post-stimulus period. In contrast, target-specific patterns in PPC were identified prior to odor onset, but these gave way to stimulus-specific patterns later in the trial.

## Pre-stimulus patterns in PPC take the form of behaviorally relevant odor templates

Although the above data provide robust evidence for olfactory predictive patterns, direct confirmation that these codes are perceptual templates or "search images" of the actual odor requires that the search pattern for a given odor (prior to stimulus onset) correlates with the actual evoked pattern for that odor (following stimulus onset). To test this idea, we hypothesized that if the observed search pattern did in fact resemble the actual pattern in response to that specific odor, then the pre-stimulus and post-stimulus activity patterns in PPC would be more correlated in trials where the stimulus matched the target than when the stimulus did not match the target. In agreement with this hypothesis, we found higher correlations between pre- and post-stimulus patterns in PPC for target/stimulus matching (vs. non-matching) trials (Fig. 5) ($T_{11} = 1.8$, $P < 0.04$; binomial test, $P < 0.003$). Thus the pre-stimulus pattern observed in PPC does in fact appear to be quite literally an odor template, that is, a stimulus-specific perceptual signature of the anticipated odor in the absence of any stimulus.

We next reasoned that if pre-stimulus odor templates exist, they should help augment olfactory perception. To this end, the strength of template formation (as indexed by the magnitude of the pre-odor correlation between same-target conditions) was regressed against performance accuracy on the olfactory search task, on a subject-wise basis. Put differently, we tested the hypothesis that subjects who generated more robust odor-target templates would be able to identify the target odor more accurately. In agreement with this prediction, the magnitude of the pre-stimulus effect in PPC was significantly correlated with task accuracy (Fig. 6) ($R = 0.64$, $P = 0.02$). Furthermore, the degree to which same-target correlations exceeded different-target correlations also correlated with task accuracy ($R = 0.66$, $P = 0.01$). By comparison, pre-stimulus ensemble patterns in APC and OFC had no demonstrable relationship to behavior ($P$'s > 0.07), indicating that the availability of predictive codes for guiding olfactory perceptual decisions specifically resides in PPC.

### A univariate fMRI index of prediction error in MDT

Recent theoretical models of sensory perception (Friston, 2005; Rao and Ballard, 1999) place high importance on hierarchical processing and prediction error: predictions reflect the top-down flow in the cortical hierarchy while prediction error reflects the bottom-up flow of afferent sensory information. Interestingly, findings from univariate fMRI analyses commonly show that an expected (vs. unexpected) percept elicits lower mean activity in sensory-related regions, a differential effect that has been attributed to prediction error signaling (Summerfield and Egner, 2009). Therefore, we conducted a complementary univariate imaging analysis to look for evidence of error signaling in our data (Fig. 7). fMRI activation in MDT was significantly reduced in response to expected trials compared to unexpected trials ($T_{11} = 2.41$, $P < 0.03$), suggesting this region may participate in generating a prediction error signal. By comparison, there were no significant differences in APC, PPC, or OFC ($P$'s > 0.2).

## Discussion

The vast majority of natural, real-world odors are encountered in the presence of other competing smells. Thus, on any given inhalation, the olfactory system faces the challenge of disambiguating salient odor objects from other odors present in the background (Linster et al., 2007). On top of this challenge, human olfactory perception is both temporally and spatially impoverished (Sela and Sobel, 2010), implying that attentional capture may be insoluble for the olfactory system (Laing and Glemarec, 1992). By utilizing fMRI multivariate analyses in conjunction with an odor search task, we were able to show that odor-specific ensemble patterns emerge prior to odor stimulation and (in PPC) reliably predict subsequent behavioral performance. These findings provide robust evidence for object-based attentional mechanisms that directly impact on odor perception.

Separation of the fMRI time-series into pre- and post-stimulus bins enabled us to identify ensemble patterns of activity both before and after odor arrival. Before the sniff and in the absence of odor, olfactory ensemble codes in APC and OFC were specific for the attended odor target, rather than being a general effect of attention, indicating that subjects can generate feature-specific information about an odor prior to its receipt. After odor onset, target-related patterns in APC and OFC persisted for up to several seconds, irrespective of the actual identity of the delivered odor. These findings indicate that the ensemble activity in APC and OFC more closely resemble what is being sought-out rather that what is being delivered to the nose. That much of the olfactory system smells what it expects rather than what it sniffs is closely reflected in our behavioral data (Fig. 2). Stimulus-specific expectations induced corresponding response biases during odor sampling: subjects misclassified a given stimulus more often when preceded by an incongruent target cue, for

example, mistaking odor B for odor A when searching for A. Similarly, reaction times were slower when subjects expected one odor but received another.

By comparison, in PPC, target-related ensemble codes before odor onset gave way to stimulus-specific codes after odor onset, whereby activity patterns more closely resembled what was delivered rather than what was being expected (Figs. 3 and 4). This response profile implies that PPC plays a highly dynamic role at the interface between sensation, expectation, and perception. Insofar as the pre-stimulus target patterns (e.g., odor A target) and the post-stimulus odor patterns (e.g., odor A stimulus) shared significant pattern overlap in PPC (Fig. 5), our findings directly show that predictive "templates" or "search images" are represented here. That the robustness of predictive coding in PPC facilitated odor perception in a stimulus-specific manner (cf. Fig. 6) further underscores the key involvement of this brain area in generating spatially distributed templates with literal functional correspondence to the actual odor patterns, in accordance with longstanding anatomical and computational models of piriform function (Freeman and Schneider, 1982; Haberly, 2001; Hasselmo et al., 1990; Ojima et al., 1984; Wilson and Stevenson, 2003).

Curiously, the relevance of persisting target patterns in APC and OFC to odor perception is unclear given that these patterns (unlike those in PPC) did not correlate with behavior. It is important to note that the subjects in our study performed relatively slowly on this task, taking between 3 and 4 seconds on average to make a decision. Therefore, it is plausible that within this post-sniff time frame, an ongoing trace in APC may have helped optimize the attentional search, without itself correlating directly with perceptual performance. Ultimately how these pre-stimulus codes in APC and OFC influence odor perception remains unresolved.

Human psychophysical and neuroimaging studies increasingly indicate that olfactory perception benefits from odor imagery and cognitive modulation. For example, imagination of a specific smell alters sniffing behavior, enhances odor detection accuracy, and elicits fMRI activations in anterior (frontal) piriform cortex and posterior OFC (Bensafi et al., 2007; Bensafi M, 2003; Djordjevic et al., 2004; Djordjevic et al., 2005). Similarly, contextual presentation of non-olfactory semantic information, such as pictures or word labels, modifies both odor perception and OFC response profiles in a stimulus-specific manner (de Araujo et al., 2005; Gottfried and Dolan, 2003; Herz and von Clef, 2001; Herz, 2003). The formation of olfactory predictive templates in APC, PPC, and OFC that precede – and in some cases persist beyond – onset of the stimulus, as shown here, represents a plausible unifying neural mechanism to explain the widespread modulatory effects of imagery and context on how an odor is perceived.

Recent theoretical perspectives make the case that predicting the appearance of particular stimulus features (i.e., "predictive coding") is mechanistically distinct from prioritizing detection of expected features due to their task relevance (i.e., "feature-based attention") (Summerfield and Egner, 2009). In the visual system for example, both processes will lead to behavioral gains in stimulus recognition, but will exert opposing effects on neural activity in regions representing the stimulus (Summerfield and Egner, 2009). Although our experimental design cannot formally distinguish between predictive coding and feature-based attention per se, the mean fMRI signal decrease in MDT following delivery of expected vs. unexpected odor stimuli (cf. Fig. 7) is compatible with predictive coding models and highlights a potential important role for this region in generating a prediction error signal. As a region that receives both top-down information from OFC and bottom-up input from PPC (Ray and Price, 1992), MDT is ideally positioned to compute an error signal by directly comparing predictions with inputs. Its reciprocal connectivity with APC, PPC,

and OFC also means that MDT would be able to communicate this error signal to these other regions for purposes of updating these predictions.

More broadly, our imaging data dovetail nicely with studies on anticipatory attention in the visual and auditory systems (Esterman and Yantis, 2010; Kastner et al., 1999; Kumar et al., 2011; Luck et al., 1997; Peelen et al., 2009; Ress et al., 2000; Summerfield et al., 2006) and imply that the brain generates predictive codes of the surrounding environment, no matter the modality. In showing that the representational content of predictive codes in PPC corresponds to the activity pattern elicited by the actual expected stimulus, our data extend earlier findings confirming mean signal changes in sensory-relevant regions. Our results generally draw out the physiological distinctions between the olfactory and visual systems, in that odor search maps in PPC are only two synapses downstream from the nasal periphery, whereas search maps in the visual modality are found much further along in the processing hierarchy (Peelen et al., 2009; Stokes et al., 2009; Summerfield et al., 2006). Nevertheless, the functional similarities between these two modalities lend further support to the notion of piriform cortex as a higher-order associative brain area, akin to visual associative areas in the inferior temporal lobe.

On a final clinical note, our data offer an intriguing potential explanation for the early olfactory dysfunction commonly described in patients with schizophrenia. Deficits in odor identification are one of the earliest symptoms to appear in schizophrenic patients, and the extent of perceptual impairment predicts poorer functional outcome (Good et al., 2010; Stevenson et al., 2011). Given that the positive symptoms of schizophrenia may be the result of a disruption in predictive coding mechanisms (Fletcher and Frith, 2009), our data may serve to unite olfactory findings in schizophrenic patients with general models of the mechanisms underlying this disease.

## Experimental Procedures

### Subjects

Thirteen subjects (6 women; age range, 19 to 23 years) participated in the fMRI study. All provided written informed consent to participate in procedures approved by the Northwestern University Institutional Review Board. Participants were screened for abnormal sense of smell or taste, history of neurological or psychiatric disease, history of nasal disorders, allergic rhinitis or sinusitis, or MRI counter-indications. One subject was excluded from analyses due to technical problems with the olfactometer.

### Odorants and odorant delivery

Odorants were delivered by an MRI-compatible, eight-channel computer-controlled air-dilution olfactometer (airflow set at 10 L/min), which permits rapid delivery of single-component odorants and binary (two-odorant) mixtures in the absence of tactile, thermal, or auditory cues, custom-built in our lab and modified from prior designs (Johnson and Sobel, 2007). Odorant stimuli consisted of methyl-3-nonenoate (A) and 1-hexanol (B), as well as a control odorant, cinnamaldehyde (C) (see Experimental Procedures), either presented individually or as binary combinations (i.e., A+B, A+C, B+C) to subjects through a nasal mask (Respironics, Murrysville, PA) that was comfortably affixed around the nose. Odorants were selected that were relatively familiar and easily discriminable from each other. All mixtures were of equal proportional concentration such that the same amount of the single compound was delivered in mixtures as when it was delivered alone, air-diluted at 40% saturation (i.e., 4 liters/min of neat-concentration odorant and 6 liters/min of air).

### Respiratory monitoring

Sniffs were recorded online during scanning via the nasal mask mask, by means of a pneumatotachograph (spirometer) that relayed respiratory-induced changes in mask pressure to an amplifier (AD Instruments, Milford, MA).

### Experimental design

Just prior to placing subjects into the scanner, we administered odorants A and B through the olfactometer and asked subjects to verbally rate the intensity of each odor on a scale from 1 to 10. The olfactometer flow settings were then adjusted until intensity ratings were matched. This also allowed subjects to become familiar with the two odors, which would be the designated target smells during the imaging experiment.

Each scanning session consisted of 6 blocks of 32 trials (11 minutes per block). Before each block, the subject was informed of the identity of the target odor, and was given a sample of the target. On each trial, subjects were prompted to sniff by a visually presented countdown ("3, 2, 1, SNIFF"), at which time an odor was presented. Subjects then responded by pushbutton to indicate whether or not the trial contained the target (Fig. 1). The target for a given run consisted of either odor A, odor B, or odor A+B. Because a 3-level ANOVA of A, B and A+B blocks indicated that behavioral performance was significantly lower on the target A+B blocks ($F_{1.60,17.62} = 5.558$; $P = 0.018$), the target A+B conditions were excluded from further analysis. Thus comparisons were restricted to target A and target B conditions, where performance did not differ ($F_{1.00,11.00} = 0.54$; $P = 0.478$).

Block and trial order were pseudorandomly balanced across subjects. On each trial, subjects received odor A alone, odor B alone, odor A+B, odor A+C, or odor B+C. The A+B stimulus condition was included so that we could look at trials in which the stimulus was identical (i.e., A+B), and only the attentional focus of the subject differed (either the A note or the B note). The A+C and B+C conditions were included as catch trials to ensure that subjects could not simply adopt a strategy to answer "yes" every time a mixture was presented. Due to time constraints, there was not a sufficient number of catch trials included to perform reliable statistical analyses of these events.

Each condition type was delivered an equal number of times per target block. Importantly, the stimulus content was identical across runs; only the identity of the target (and therefore the attentional search focus of the subject) differed across blocks. In this way, we were able to look for attention-driven sensory-specific responses by comparing the fMRI time series in same-target vs. different-target conditions.

Each scanning session also included a $7^{th}$ block of an "odor localizer" task, consisting of 18 trials of an odor detection task (Li et al., 2008). Results from this scan were used only for voxel selection in subsequent analyses.

### Acquisition parameters and defining ROIs

All fMRI data were collected on a Siemens Trio 3T MRI scanner, using a twelve-channel head coil and an integrated parallel acquisition technique known as GRAPPA (GeneRalized Autocalibrating Partially Parallel Acquisition) to improve signal recovery in medial temporal and basal frontal regions (Li et al., 2006). Imaging parameters included: TR, 1.51 s; TE, 20 ms; slice thickness, 2 mm; gap, 1 mm; in-plane resolution, 1.72 × 1.72 mm; field of view, 220 × 220 mm, matrix size, 128 × 120 mm. Image acquisition was tilted at 30° to further reduce susceptibility artifact in olfactory areas. A total of 24 slices per volume were collected to ensure adequate coverage of olfactory brain regions. In addition to the functional scans, a T1-weighted whole-brain anatomical scan at 1-$mm^3$ resolution was

acquired for the purpose of outlining regions of interest (ROI). An additional lower resolution anatomical scan was acquired with the same slice protocol as the functional scans, to aid with realignment of the functional data to the high resolution whole-brain anatomical image.

Data were analyzed using mrVista (http://white.stanford.edu/software/) and Matlab. First, we defined olfactory cortical areas by outlining ROIs of anterior piriform cortex (APC), posterior piriform cortex (PPC), mediodorsal thalamus (MDT), and orbitofrontal cortex (OFC) on each subject's T1-weighted anatomical scan, with reference to a human brain atlas (Mai et al., 1997). Following our prior techniques (Howard et al., 2009), the anatomical landmark used to delineate the caudal extent of APC from the rostral extent of PPC was defined as the location in the coronal T1 sections where the medial temporal and basal frontal lobes first join together. Construction of the ROIs was performed before any further analysis, and in the absence of functional results. Because one subject's acquisition did not fully cover MDT, this particular ROI could not be analyzed for that subject.

In a subsequent step, we set out to functionally restrict the ROIs to voxels that were activated during the localizer scan. First, the time-series in each ROI were converted into percent signal change by dividing each by its mean response and multiplying by 100. Then, for each subject we calculated an activation mask to filter out voxels for which we had no signal. We produced images of the average response across all time points at each voxel. Because voxels in gray and white matter have a significantly different mean response than voxels in bone or air, we were able to filter voxels based on their mean response to include only voxels for which we had signal (Zelano et al., 2007). This eliminated voxels that were in regions of high susceptibility, particularly near the ventral frontal and temporal surface of cortex.

Second, for each subject we produced a noise mask similar to the first, which calculated the standard deviation of the response at each voxel. This mask also discriminated between regions of high susceptibility and brain tissue, and further excluded voxels with high noise, such as voxels on large blood vessels.

Third, we restricted each subject's anatomical ROI to those voxels that responded to odor stimulation on the localizer task. This was calculated by correlating the response at each voxel following an odorant event with a standard hemodynamic response function used by mrVista software. By calculating the correlation of each voxel to an expected hemodynamic response function, and the statistical significance of this correlation, we were able to produce a statistical parametric map of the responsiveness of each voxel to odorants. To limit the anatomical ROIs to "odorant" responsive voxels, we excluded all voxels whose correlation to the hemodynamic response function had a statistical significance value higher than $P = 0.01$. Subsequent analysis proceeded with these functionally restricted ROIs. As indicated in Supplemental Information, despite differences in the numbers of voxels included in each ROI, there was no evidence that the significant patterns were more likely to emerge for ROIs containing higher numbers of voxels (Fig. S2).

### Time-series analysis

The single-trial fMRI time-series in each voxel of each ROI for each condition were first baseline-corrected by subtracting the mean fMRI activity in the interval from 3 TRs pre-sniff to 1 TR pre-sniff. Note that this procedure had no effect on the spatiotemporal profile of the response. We then averaged across trials, and defined two intervals of interest (time 0 being stimulus onset) in each event-related time series, one extending from −3 TR – 0 TR (pre-stimulus bin) and another from 3 TR – 6 TR (post-stimulus bin). Our rationale for defining these bins was principally based on including as many pre-stimulus TRs (4 TRs, or

~6 s) as was reasonably possible before the pre-stimulus bin began to encroach on the end of the previous trial. The post-stimulus bin was designed to span the main fMRI response peak, which generally occurs 4-5 seconds after the stimulus onset, with a 4-TR width set to ensure that the pooled variance over the interval was matched for pre- and post-bins. We then created pre-stimulus and post-stimulus vectors for each subject containing the mean activity in the two time-bins for each voxel. Note that increasing the post-bin width by an additional 2 TRs did not significantly alter the main findings.

To compare the different conditions, we computed linear correlation coefficients (*R* values) between the voxel vectors for the different conditions for each subject, resulting in a single correlation coefficient per subject, per ROI, and per condition comparison. To look for effects of target and stimulus, we hypothesized that the ensemble pattern would be more correlated between *same-target/different stimulus* conditions than between *different-target/ same stimulus* conditions in brain regions encoding the odor search target. Note that all same-target conditions coincided with different-stimulus conditions, and all same-stimulus conditions coincided with different-target conditions. In this way, we were able to look for both target and stimulus effects in a single comparison in the pre- and post-stimulus bins.

In a multivariate analysis to establish evidence for stimulus-specific predictive templates (Fig. 5), pre-stimulus *target* patterns were compared to post-stimulus *odor* patterns in PPC. Because a pre-stimulus pattern could theoretically be compared to a post-stimulus pattern from the same trial, consequently introducing analysis confounds, we made sure that pre- and post-stimulus comparisons were always drawn from independent trials. For example, if a pre-stimulus target "A" pattern was derived from the **A**|A condition, then the post-stimulus odor "A" pattern for comparison would have been derived from the **A**|B condition (and never from the **A**|A condition).

Regions of interest included APC, PPC, OFC and MDT. Because results did not differ between the left and right ROI for each region (*P*'s > 0.2), results are reported collapsed across sides. For each ROI, the data were entered into 3-way repeated-measure ANOVAs with "target run" (odor A or odor B), "pattern type" (target-related or stimulus-related), and "time" (pre- or post-stimulus bin) as factors. Use of a repeated-measures ANOVA, which is based on within-subject variance across conditions, effectively eliminated potential confounds that might arise from between-subject variance.

A separate univariate fMRI analysis was also conducted in an effort to identify brain areas involved in prediction error coding. To this end, the mean time-series for each ROI was computed by averaging across all voxels and trials per condition, separately for each subject. The maximum value over a window from 3 to 6 TRs post-sniff was then computed for each subject for each ROI for each condition, and comparison between expected and unexpected conditions was achieved through paired t-tests.

Statistical significance criterion for all comparisons was set at $P < 0.05$, using either paired t-tests (comparison of two conditions) or repeated-measures ANOVA (comparison of three or more conditions), as appropriate.

## Supplementary Material

Refer to Web version on PubMed Central for supplementary material.

## Acknowledgments

We thank Katherina Hauner, Joel Mainland, and M.-Marsel Mesulam for helpful comments, and Katie Phillips for assistance in collecting data. Supported by the National Institute on Deafness and Other Communication Disorders grants 1R01DC010014 and K08DC007653 (to J.A.G.) and F32DC010530-01A1 (to C.Z).

## References

1. Bensafi M, Sobel N, Khan RM. Hedonic-specific activity in piriform cortex during odor imagery mimics that during odor perception. J Neurophysiol. 2007; 98:3254–3262. [PubMed: 17913994]
2. Bensafi M,PJ, Pouliot S, Mainland J, Johnson B, Zelano C, Young N, Bremner E, Aframian D, Khan R, Sobel N. Olfactomotor activity during imagery mimics that during perception. Nat Neurosci. 2003; 6:1142–1144. [PubMed: 14566343]
3. de Araujo IE, Rolls ET, Velazco MI, Margot C, Cayeux I. Cognitive modulation of olfactory processing. Neuron. 2005; 46:671–679. [PubMed: 15944134]
4. Djordjevic J, Zatorre RJ, Petrides M, Jones-Gotman M. The mind's nose: Effects of odor and visual imagery on odor detection. Psychol Sci. 2004; 15:143–148. [PubMed: 15016284]
5. Djordjevic J, Zatorre RJ, Petrides M, Boyle JA, Jones-Gotman M. Functional neuroimaging of odor imagery. Neuroimage. 2005; 24:791–801. [PubMed: 15652314]
6. Esterman M, Yantis S. Perceptual expectation evokes category-selective cortical activity. Cereb Cortex. 2010; 20:1245–1253. [PubMed: 19759124]
7. Fletcher PC, Frith CD. Perceiving is believing: a Bayesian approach to explaining the positive symptoms of schizophrenia. Nat Rev Neurosci. 2009; 10:48–58. [PubMed: 19050712]
8. Freeman WJ. EEG analysis gives model of neuronal template-matching mechanism for sensory search with olfactory bulb. Biol Cybern. 1979; 35:221–234. [PubMed: 526484]
9. Freeman WJ. A physiological hypothesis of perception. Perspect Biol Med. 1981; 24:561–592. [PubMed: 7027172]
10. Freeman WJ, Schneider W. Changes in spatial patterns of rabbit olfactory EEG with conditioning to odors. Psychophysiology. 1982; 19:44–56. [PubMed: 7058239]
11. Freeman WJ. The physiological basis of mental images. Biol Psychiatry. 1983; 18:1107–1125. [PubMed: 6317064]
12. Friston K. Learning and inference in the brain. Neural Netw. 2003; 16:1325–1352. [PubMed: 14622888]
13. Friston K. A theory of cortical responses. Philos Trans R Soc Lond B Biol Sci. 2005; 360:815–836. [PubMed: 15937014]
14. Friston KJ. Models of brain function in neuroimaging. Annu Rev Psychol. 2005; 56:57–87. [PubMed: 15709929]
15. Good KP, Tibbo P, et al. An investigation of a possible relationship between olfactory identification deficits at first episode and four-year outcomes in patients with psychosis. Schizophr Res. 2010; 124:60–65. [PubMed: 20692126]
16. Gottfried JA, Dolan RJ. The nose smells what the eye sees: crossmodal visual facilitation of human olfactory perception. Neuron. 2003; 39:375–386. [PubMed: 12873392]
17. Gottfried JA, Winston JS, Dolan RJ. Dissociable codes of odor quality and odorant structure in human piriform cortex. Neuron. 2006; 49:467–479. [PubMed: 16446149]
18. Gottfried JA. Central mechanisms of odour object perception. Nat Rev Neurosci. 2010; 11:628–641. [PubMed: 20700142]
19. Haberly LB. Neuronal circuitry in olfactory cortex - anatomy and functional implications. Chemical Senses. 1985; 10:219–238.
20. Haberly LB. Parallel-distributed processing in olfactory cortex: New insights from morphological and physiological analysis of neuronal circuitry. Chemical Senses. 2001; 26:551–576. [PubMed: 11418502]
21. Hasselmo ME, Wilson MA, Anderson BP, Bower JM. Associative memory function in piriform (olfactory) cortex: computational modeling and neuropharmacology. Cold Spring Harb Symp Quant Biol. 1990; 55:599–610. [PubMed: 2132840]

22. Herz RS, von Clef J. The influence of verbal labeling on the perception of odors: evidence for olfactory illusions? Perception. 2001; 30:381–391. [PubMed: 11374206]
23. Herz RS. The effect of verbal context on olfactory perception. J Exp Psychol Gen. 2003; 132:595–606. [PubMed: 14640850]
24. Howard JD, Plailly J, Grueschow M, Haynes JD, Gottfried JA. Odor quality coding and categorization in human posterior piriform cortex. Nat Neurosci. 2009; 12:932–938. [PubMed: 19483688]
25. Illig KR, Haberly LB. Odor-evoked activity is spatially distributed in piriform cortex. Journal of Comparative Neurology. 2003; 457:361–373. [PubMed: 12561076]
26. Johnson BN, Sobel N. Methods for building an olfactometer with known concentration outcomes. J Neurosci Methods. 2007; 160:231–245. [PubMed: 17081618]
27. Kastner S, Pinsk MA, De Weerd P, Desimone R, Ungerleider LG. Increased activity in human visual cortex during directed attention in the absence of visual stimulation. Neuron. 1999; 22:751–761. [PubMed: 10230795]
28. Kay LM, Freeman WJ. Bidirectional processing in the olfactory-limbic axis during olfactory behavior. Behav Neurosci. 1998; 112:541–553. [PubMed: 9676972]
29. Kay LM, Stopfer M. Information processing in the olfactory systems of insects and vertebrates. Semin Cell Dev Biol. 2006; 17:433–442. [PubMed: 16766212]
30. Kumar S, Sedley W, et al. Predictive Coding and Pitch Processing in the Auditory Cortex. J Cogn Neurosci. 2011
31. Laing DG, Glemarec A. Selective attention and the perceptual analysis of odor mixtures. Physiol Behav. 1992; 52:1047–1053. [PubMed: 1484860]
32. Li W, Luxenberg E, Parrish T, Gottfried JA. Learning to smell the roses: experience-dependent neural plasticity in human piriform and orbitofrontal cortices. Neuron. 2006; 52:1097–1108. [PubMed: 17178411]
33. Li W, Howard JD, Parrish TB, Gottfried JA. Aversive learning enhances perceptual and cortical discrimination of indiscriminable odor cues. Science. 2008; 319:1842–1845. [PubMed: 18369149]
34. Linster C, Henry L, Kadohisa M, Wilson DA. Synaptic adaptation and odor-background segmentation. Neurobiol Learn Mem. 2007; 87:352–360. [PubMed: 17141533]
35. Luck SJ, Chelazzi L, Hillyard SA, Desimone R. Neural mechanisms of spatial selective attention in areas V1, V2, and V4 of macaque visual cortex. J Neurophysiol. 1997; 77:24–42. [PubMed: 9120566]
36. Mai, J.; Assheuer, J.; Paxinos, G. Atlas of the human brain. Academic Press; London: 1997.
37. Martin C, Gervais R, Chabaud P, Messaoudi B, Ravel N. Learning-induced modulation of oscillatory activities in the mammalian olfactory system: the role of the centrifugal fibres. J Physiol Paris. 2004; 98:467–478. [PubMed: 16274975]
38. McMains SA, Fehd HM, Emmanouil TA, Kastner S. Mechanisms of feature- and space-based attention: response modulation and baseline increases. J Neurophysiol. 2007; 98:2110–2121. [PubMed: 17671104]
39. Mesulam M. Representation, inference, and transcendent encoding in neurocognitive networks of the human brain. Ann Neurol. 2008; 64:367–378. [PubMed: 18991346]
40. Mumford D. On the computational architecture of the neocortex. II. The role of cortico-cortical loops. Biol Cybern. 1992; 66:241–251. [PubMed: 1540675]
41. Ojima H, Mori K, Kishi K. The trajectory of mitral cell axons in the rabbit olfactory cortex revealed by intracellular HRP injection. J Comp Neurol. 1984; 230:77–87. [PubMed: 6096415]
42. Peelen MV, Fei-Fei L, Kastner S. Neural mechanisms of rapid natural scene categorization in human visual cortex. Nature. 2009; 460:94–97. [PubMed: 19506558]
43. Plailly J, Howard JD, Gitelman DR, Gottfried JA. Attention to odor modulates thalamocortical connectivity in the human brain. J Neurosci. 2008; 28:5257–5267. [PubMed: 18480282]
44. Porter J, Anand T, Johnson B, Khan RM, Sobel N. Brain mechanisms for extracting spatial information from smell. Neuron. 2005; 47:581–592. [PubMed: 16102540]
45. Rao RP, Ballard DH. Predictive coding in the visual cortex: a functional interpretation of some extra-classical receptive-field effects. Nat Neurosci. 1999; 2:79–87. [PubMed: 10195184]

46. Ray JP, Price JL. The organization of the thalamocortical connections of the mediodorsal thalamic nucleus in the rat, related to the ventral forebrain-prefrontal cortex topography. J Comp Neurol. 1992; 323:167–197. [PubMed: 1401255]
47. Rennaker RL, Chen CF, Ruyle AM, Sloan AM, Wilson DA. Spatial and temporal distribution of odorant-evoked activity in the piriform cortex. J Neurosci. 2007; 27:1534–1542. [PubMed: 17301162]
48. Ress D, Backus BT, Heeger DJ. Activity in primary visual cortex predicts performance in a visual detection task. Nat Neurosci. 2000; 3:940–945. [PubMed: 10966626]
49. Sabri M, Radnovich AJ, Li TQ, Kareken DA. Neural correlates of olfactory change detection. Neuroimage. 2005; 25:969–974. [PubMed: 15808997]
50. Schoenbaum G, Eichenbaum H. Information coding in the rodent prefrontal cortex. I. Single-neuron activity in orbitofrontal cortex compared with that in pyriform cortex. J Neurophysiol. 1995; 74:733–750. [PubMed: 7472378]
51. Sela L, Sobel N. Human olfaction: a constant state of change-blindness. Exp Brain Res. 2010; 205:13–29. [PubMed: 20603708]
52. Sobel N, Prabhakaran V, et al. Sniffing and smelling: separate subsystems in the human olfactory cortex. Nature. 1998; 392:282–286. [PubMed: 9521322]
53. Spence C, McGlone FP, Kettenmann B, Kobal G. Attention to olfaction. A psychophysical investigation. Exp Brain Res. 2001; 138:432–437. [PubMed: 11465740]
54. Spors H, Grinvald A. Spatio-temporal dynamics of odor representations in the mammalian olfactory bulb. Neuron. 2002; 34:301–315. [PubMed: 11970871]
55. Stettler DD, Axel R. Representations of odor in the piriform cortex. Neuron. 2009; 63:854–864. [PubMed: 19778513]
56. Stevenson RJ, Wilson DA. Odour perception: an object-recognition approach. Perception. 2007; 36:1821–1833. [PubMed: 18283932]
57. Stevenson RJ, Langdon R, McGuire J. Olfactory hallucinations in schizophrenia and schizoaffective disorder: a phenomenological survey. Psychiatry Res. 2011; 185:321–327. [PubMed: 20727597]
58. Stokes M, Thompson R, Nobre AC, Duncan J. Shape-specific preparatory activity mediates attention to targets in human visual cortex. Proc Natl Acad Sci U S A. 2009; 106:19569–19574. [PubMed: 19887644]
59. Summerfield C, Egner T, et al. Predictive codes for forthcoming perception in the frontal cortex. Science. 2006; 314:1311–1314. [PubMed: 17124325]
60. Summerfield C, Egner T. Expectation (and attention) in visual cognition. Trends Cogn Sci. 2009; 13:403–409. [PubMed: 19716752]
61. Sylvester CM, Shulman GL, Jack AI, Corbetta M. Anticipatory and stimulus-evoked blood oxygenation level-dependent modulations related to spatial attention reflect a common additive signal. J Neurosci. 2009; 29:10671–10682. [PubMed: 19710319]
62. Takiguchi N, Okuhara K, Kuroda A, Kato J, Ohtake H. Performance of mice in discrimination of liquor odors: behavioral evidence for olfactory attention. Chem Senses. 2008; 33:283–290. [PubMed: 18178544]
63. Veldhuizen MG, Bender G, Constable RT, Small DM. Trying to detect taste in a tasteless solution: modulation of early gustatory cortex by attention to taste. Chem Senses. 2007; 32:569–581. [PubMed: 17495173]
64. Wald A, Wolfowitz J. Bayes Solutions of Sequential Decision Problems. Proc Natl Acad Sci U S A. 1949; 35:99–102. [PubMed: 16588867]
65. Wilson DA, Stevenson RJ. The fundamental role of memory in olfactory perception. Trends Neurosci. 2003; 26:243–247. [PubMed: 12744840]
66. Zelano C, Bensafi M, et al. Attentional modulation in human primary olfactory cortex. Nat Neurosci. 2005; 8:114–120. [PubMed: 15608635]
67. Zelano C, Montag J, Khan R, Sobel N. A specialized odor memory buffer in primary olfactory cortex. PLoS One. 2009; 4:e4965. [PubMed: 19305509]

68. Zelano CM, Montag J, Johnson B, Khan R, Sobel N. Dissociated representations of irritation and valence in human primary olfactory cortex. J Neurophysiol. 2007

Highlights

- Odor ensembles in APC and OFC reflect what is sought, rather than what is delivered.
- PPC patterns evolve from predictive templates to odor codes after stimulus onset
- The strength of template formation in PPC predicts olfactory perceptual performance
- Neural access to both target and stimulus codes may help resolve odor ambiguity

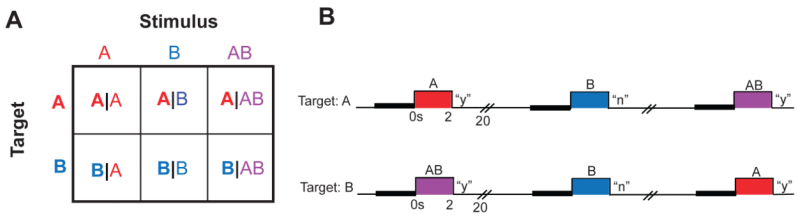


**Figure 1.**

Experimental design and behavioral results. **A**. Subjects took part in an olfactory attentional search paradigm that conformed to a two-way factorial design in which either odor target or odorant stimulus was varied. **B.** At the start of each fMRI run, subjects were informed whether the target smell would be odor A or odor B for that run. On a given trial, a countdown cue began 3 seconds prior to sniff (thick black bar), then one of the odor stimuli was presented and subjects indicated whether or not the assigned target odor was present in the stimulus (“y” or “n”).

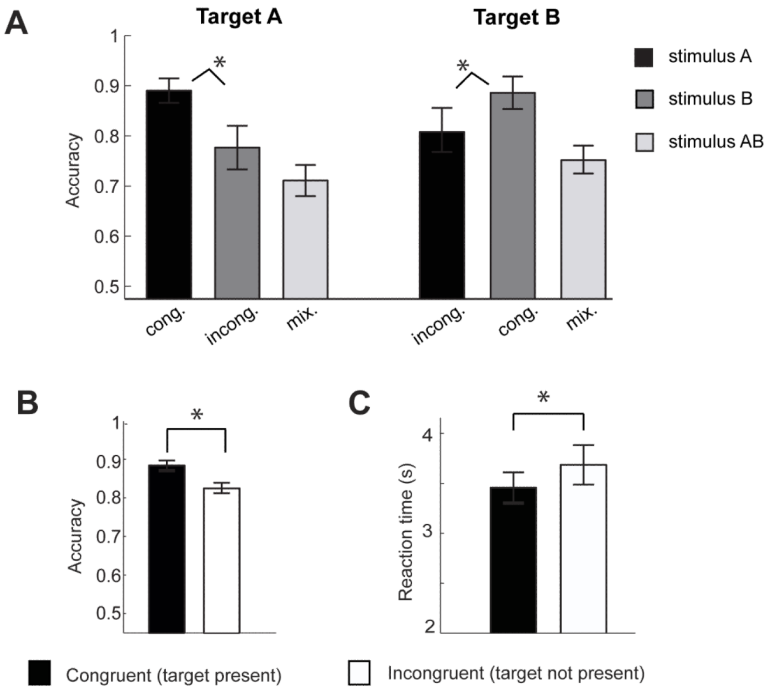


**Figure 2.**

Behavioral results. **A.** Overall detection accuracy for the target odor did not significantly differ across A and B runs, though performance was better with A and B stimuli than with the AB stimulus mixture (mix.). A cross-over interaction was observed, in which subjects were more accurate on target A runs when the stimulus was A (congruent condition; cong.) rather than B (incongruent condition; incong.), and were more accurate on target B runs when the stimulus was B (cong.) rather than A (incong.). **B.** Performance accuracy, collapsed across A and B runs, was significantly higher when the target was present in the stimulus (cong.) compared to when the target was not present (incong.). **C.** Reaction times followed a similar profile, such that subjects were faster for congruent trials compared to incongruent trials. *, $P < 0.05$.

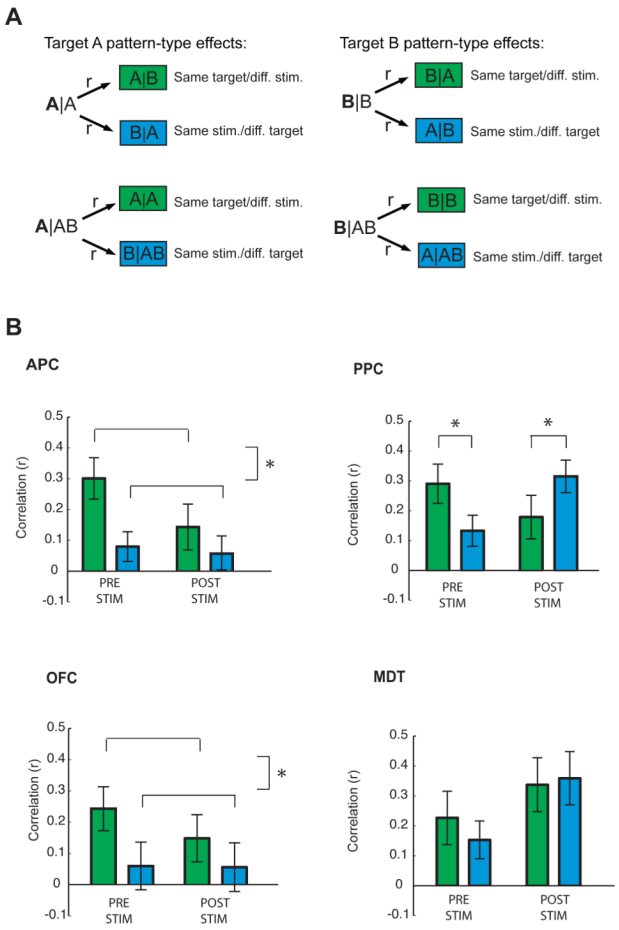


**Figure 3.**

Odor-specific predictive codes in the olfactory system. **A.** We made use of a single comparison (same target/different stimulus vs. same stimulus/different target) to look for both target-related effects (green) and stimulus-related effects (blue). These comparisons were computed for all target A runs (**A**|A compared to **A**|B vs. **B**|A; **A**|AB compared to **A**|A vs. **B**|AB) and for all target B runs (**B**|B compared to **B**|A vs. **A**|B; **B**|AB compared to **B**|B vs. **A**|AB), both before and after odor onset. **B.** Target- and stimulus-related effects were computed by testing whether multivoxel correlations between same-target/different-stimulus conditions (green bars) differed from different-target/same-stimulus conditions (blue bars). Same-target correlations significantly exceeded different-target correlations in APC and OFC both before and after stimulus arrival. In PPC, same-target conditions were more correlated than different-target conditions before stimulus onset, but same-stimulus conditions were more correlated than different-stimulus conditions after stimulus onset. *, $P < 0.05$. Error bars denote between-subject S.E.M. for each comparison.

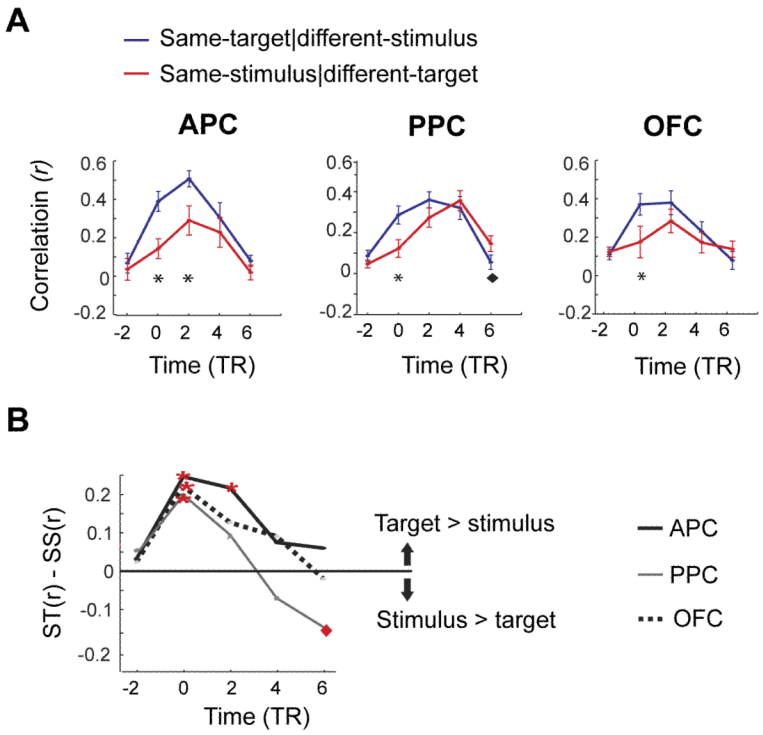


**Figure 4.**

The temporal evolution of predictive codes and stimulus representations differs across olfactory cortical regions. **A.** In all three regions, correlations increase prior to stimulus arrival for same-target conditions (blue lines), and remain elevated over same-stimulus conditions (red lines) in APC and OFC. In contrast, the correlation time-course in PPC exhibits two peaks: an early peak for same-target conditions, and then a later peak for same-stimulus conditions, reflecting the observed double dissociation between pattern type (target vs. stimulus) and time (pre vs post) in this region. Each plotted point represents the mean over two consecutive TRs. Black stars indicate time-points where same-target correlations exceed same-stimulus correlations; black diamonds indicate time-points where same-stimulus correlations exceed same-target correlations (at $P < 0.05$). **B.** To better visualize these effects, the correlation difference between the blue and red lines in panel A was plotted for each region at each time-point (ST(r), same-target r-value; and SS(r), same-stimulus r-value). A shift in pattern coding from target to stimulus is apparent in PPC at the crossing of the x-axis. Red stars, significant target-related effect; red diamonds, significant stimulus-related effect; $P < 0.05$.

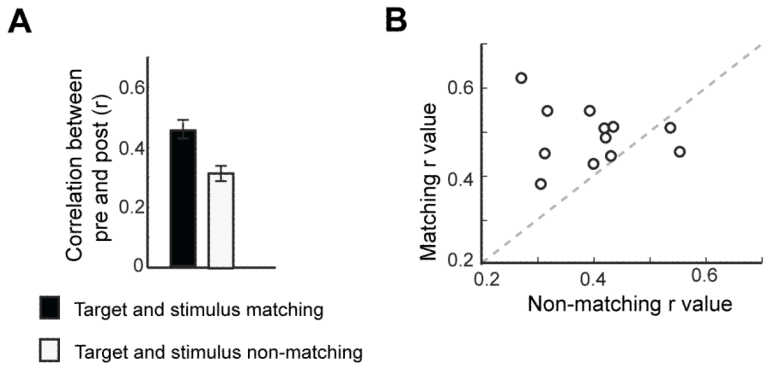


**Figure 5.**

Predictive odor templates in PPC resemble the stimulus response to the target smell. (**A**) In PPC, pre-stimulus target-specific ensemble patterns more closely resembled post-stimulus odor patterns when the target matched the stimulus (e.g., **A**|A vs. **B**|A) compared to when it did not (e.g., **A**|A vs. **A**|B). Subject-averaged correlations for matching and non-matching conditions, averaged across both A and B targets, are shown (means ± s.e.m.). (**B**) A scatterplot of matching versus non-matching conditions in PPC indicates that the pre-stimulus target template was more highly correlated to matching (vs. non-matching) post-stimulus odor representations for 10/12 subjects.

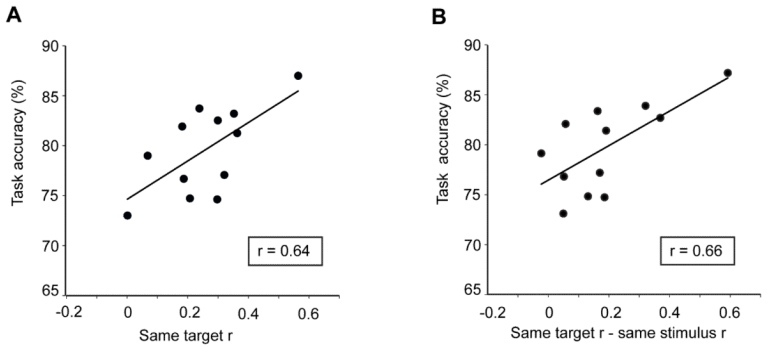


**Figure 6.**

Feature-specific pre-stimulus patterns augment olfactory perception. (**A**) The strength of pattern correlation between same-target conditions in PPC predicted identification accuracy on the odor search task. (**B**) The extent to which PPC ensemble overlap was greater for same-target conditions than for different-target conditions was also positively correlated with performance, on a subject-by-subject basis. Note, each dot represents one subject.

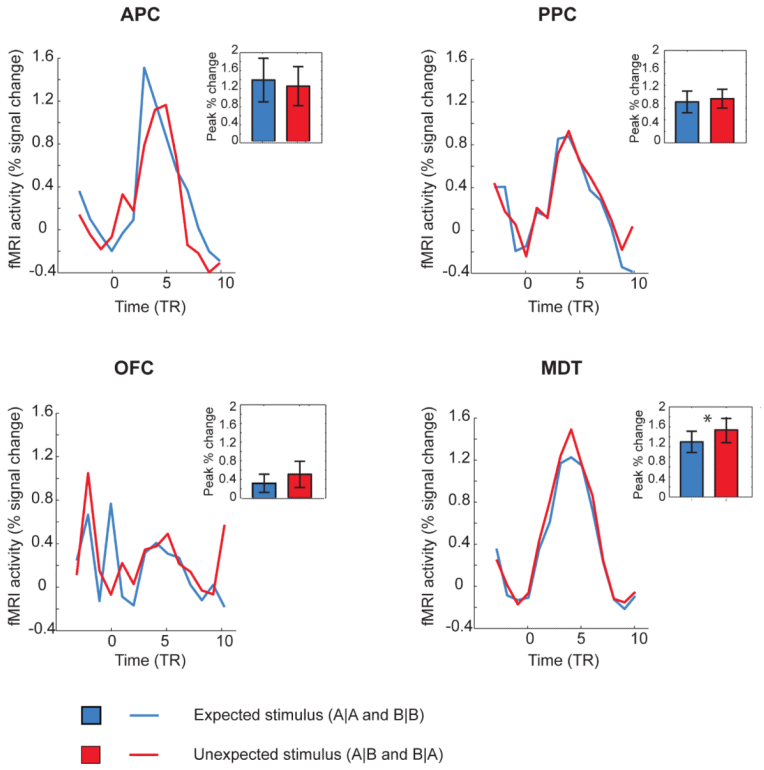


**Figure 7.**

Univariate fMRI analysis reveals that the mean level of odor-evoked activity in MDT is reduced in response to an expected or predictable stimulus. The group-averaged mean percent signal change is plotted over time within each ROI. In MDT, unexpected conditions elicited a higher response magnitude than did expected conditions.